HHS Public Access

Author manuscript

J Immunol. Author manuscript; available in PMC 2019 April 15.

Published in final edited form as:

J Immunol. 2018 April 15; 200(8): 2777–2785. doi:10.4049/jimmunol.1701542.

RGC32 promotes bleomycin-induced systemic sclerosis in a murine disease model by modulating classically activated macrophage function[1]

Chenming Sun and **Shi-You Chen***

Department of Physiology & Pharmacology, University of Georgia, Athens, GA 30602

Abstract

Systemic sclerosis (SSc) is a multisystem autoimmune disorder characterized by inflammation and fibrosis in the skin and internal organs. Previous studies indicate that inflammatory cells and cytokines play essential roles in the pathogenesis of SSc. However, the mechanisms underlying inflammation driving SSc development are not fully understood. In the present study, we show that response gene to complement 32 (RGC32) is abundantly expressed in mouse macrophages at the early stage of bleomycin-induced murine model of SSc. Importantly, RGC32 is required to induce the inflammatory response during the onset of SSc as RGC32 deficiency in mice significantly ameliorates skin and lung sclerosis and inhibits the expression of inflammatory mediators iNOS and IL-1β in macrophages. RGC32 appears to be a novel regulator for the differentiation of classically activated macrophage. IFNγ and LPS stimulation induces RGC32 expression in primary peritoneal macrophages (PEMs) and bone marrow derived macrophages (BMDMs). RGC32 deficiency impairs the polarization of classically activated macrophages and attenuates iNOS and IL-1β production. Mechanistically, RGC32 interacts with NF-κB proteins and promotes iNOS and IL-1β expression by binding to their promoters. Collectively, our data reveal that RGC32 promotes the onset of SSc by regulating the inflammatory response of classically activated macrophages, serving RGC32 as a promising therapeutic target for treating systemic sclerosis.

Keywords

Response gene to complement 32; classically activated macrophage; systemic sclerosis; NF-κB

Introduction

Systemic sclerosis (SSc) is a multisystem autoimmune disease characterized by fibrosis of the skin and other internal organs including lung, gastrointestinal tract, heart, and kidney, accompanied by abnormalities in innate and adaptive immunity (1, 2). Although the etiology of SSc remains uncertain, several advances have been made in understanding the immune response involved in SSc development, including immunological activation with infiltration

[1]This work was supported by grants from National Institutes of Health (HL119053, HL123302, and HL135854).

***Corresponding author:** Shi-You Chen, PhD, Department of Physiology & Pharmacology, The University of Georgia, 501 D.W. Brooks Drive, Athens, GA 30602, Tel: 706-542-8284, Fax: 706-542-3015, sc229@uga.edu.

Disclosures: None

of mononuclear immune cells, microvascular endothelium injury by immune cells, and fibroblast activation in organs by pro-inflammatory cytokines, which leads to excessive deposition of extracellular matrix (3, 4). In particular, recent studies highlighted the presence of macrophages as a prerequisite for SSc, as shown in bleomycin-induced dermal and lung fibrosis in nude, rag-deficient, or severe Combined Immunodeficiency (SCID) mice (5–7).

Macrophages, as the key regulator cells in the immune system, display diverse plasticity and physiology, giving rise to different populations with distinct functions. The classically activated macrophages (M1) stimulated by interferon-gamma (IFNγ) and lipopolysaccharides (LPS) are a macrophage population with strong capacity of secreting high levels of pro-inflammatory cytokines including interleukin-1β (IL-1β) and nitric oxide (NO) depending on inducible nitric oxide synthase (iNOS) through nuclear factor kappa-light-chain-enhancer of activated B cells (NF-κB) signaling pathway (8–10). The mononuclear inflammatory cells and pro-inflammatory cytokines such as IL-1β and tumor necrosis factor α (TNFα) are significantly higher in the bronchoalveolar lavage fluid and peripheral blood of SSc patients (11). In addition, SSc patients show enhanced NF-κB activity (12) and increased expression of a cluster of interferon (IFN)-regulated genes (13). Although these findings suggest a potential function of macrophages in SSc, the precise roles of inflammatory macrophages and NF-κB signaling in the pathogenesis of SSc remain poorly defined. The alternatively activated macrophages or M2 macrophages, on the other hand, are stimulated by interleukin-4 (IL4) to promote the arginase activity (8). A high abundance of M2 macrophages are observed in SSc patient skins (14), suggesting M2 macrophages also play a role in the development of the SSc.

Response gene to complement 32 (RGC32) is a cell cycle regulator involved in cell cycle regulation, cell migration and differentiation (15–17). We have previously reported that RGC32-deficient macrophages exhibit decreased phagocytosis (18). RGC32 expression is up-regulated in colony-stimulating factor (M-CSF)- and/or IL-4-dependent tumor-associated macrophages (TAMs) (19). In addition, by interacting with Smad3, RGC32 promotes fibroblast activation in renal tubulointerstitial fibrosis (20). However, the regulatory role of RGC32 in M1 macrophage differentiation, inflammatory response, especially in SSc development remains to be determined.

In the present study, we found that RGC32 played a critical role in bleomycin-induced onset of SSc. RGC32 deficiency significantly ameliorated both skin and lung sclerosis. RGC32 mediated SSc development mainly by promoting the polarization of classically activated macrophage and inflammatory response by interacting with NF-κB and enhancing iNOS and IL-1β gene expression via binding to their promoters.

Materials and methods

Mice

Both male and female mice were used in the studies. RGC32 deficient (RGC32−/−) mice on the C57BL/6 background were generated and genotyped as described previously (21). Wild-type littermates were used as controls. All the animals were housed in compliance with the

Principles of Laboratory Animal Care. Animal surgical procedures were approved by the Institutional Animal Care and Use Committee of the University of Georgia.

Cytokines and reagents

Bleomycin was purchased from Thermo Fisher Scientific. The following antibodies were used in Western blot and immunofluorescent staining. RGC32 polyclonal antibody was produced by Proteintech Group, Inc. (Chicago, IL) (16). Collagen type I alpha 1 (COL1A1) (D-13) and Lamin B (C-20) were obtained from Santa Cruz Biotechnology. Inducible nitric oxide synthase (iNOS) (4E5), Arginase (4E6) and CD3 were purchased from Abcam. IL-1β (3A6), NF-κB p65 (D14E12), Phospho-NF-κB p65 (Ser536), nuclear factor of kappa light polypeptide gene enhancer in B-cells inhibitor (IκB) (44D4) and Phospho-IκB (Ser32) were from Cell Signaling Technology. Glyceraldehyde 3-phosphate dehydrogenase (GAPDH) was from Proteintech. F4/80 (BM8) was from BioLegend. Nuclei were stained with 4, 6-diamidino-2-phenylindole (DAPI, Vector Laboratories, Inc.). The secondary antibodies were from Cell Signaling Technology. M-CSF and IFNγ were purchased from R&D Systems. M-CSF was used at 10 ng/mL, and IFNγ was used at 100 ng/mL respectively. LPS was obtained from Sigma (Sigma-Aldrich, St. Louis, MO, USA) and used at 100 ng/mL.

Bleomycin-induced murine model of SSc

To induce skin fibrosis, bleomycin (0.02U) dissolved in phosphate buffered saline (PBS) was injected subcutaneously into a single location on the back of the mice daily for 28 days. To induce pulmonary fibrosis, bleomycin (0.2U) was applied intranasally once, and the mice were euthanized after 24 days. PBS was used as control in both models. The skin or lung tissues were isolated for further analyses.

Peritoneal macrophages (PEMs) and bone marrow-derived macrophages (BMDMs)

Mouse PEMs were obtained from the peritoneum by PBS flushing and cultured in Dulbecco's Modified Eagle's medium (DMEM) medium as previously described (22). Briefly, peritoneal cells were flushed out from peritoneal cavity using cold PBS and cultured in Dulbecco's Modified Eagle's medium (DMEM) medium supplemented with 10% heat-inactivated FBS in a humidified CO2 incubator at 37 °C for 2 hours. The adherent cells constituting more than 90% of macrophages were harvested.

BMDM were generated from bone marrow by M-CSF induction as described previously (22). Bone marrow was aseptically flushed out from the tibiae and femurs of euthanized mice and depleted of red blood cells using red blood cell lysis buffer (Roche Corporation). The cells were first incubated in DMEM medium in a cell culture dish at 37°C for 2 hours to remove macrophages. The non-adherent cells were re-suspended in DMEM medium supplemented with 10% heat-inactivated FBS, 100 U/ml penicillin, 100 mg/ml stereptomycin, 2mM L-Glutamine (Thermo Fisher Scientific), and 10 ng/ml M-CSF and cultured for 7 days. Non-adherent cells were removed and M-CSF-conditioned medium was changed on day 3 and day 5. To acquire M1 macrophages, macrophages were stimulated with 100 ng/mL IFNγ and 100 ng/ml LPS for 3 hours for mRNA analysis or 6 h for protein assays.

Bone marrow chimeras

Bone marrow cells (BMCs) from 8-wk-old wild type littermates (WT) and RGC32−/− mice were prepared respectively. 1×10^7 cells were injected into the tail vein of lethally irradiated 8-wk-old WT recipient mice to generate full chimeras as described (23). 8 weeks after reconstitution, recipient mice were treated with bleomycin or PBS. Mice were euthanized at indicated time points, and the skin or lung samples were isolated for further analyses.

Histopathology and immunofluorescent staining

Skin and lung tissues were fixed in 4% paraformaldehyde (PFA) and embedded in paraffin. Tissue sections (5 μm thick) were stained with hematoxylin-eosin (H&E) or Masson's trichrome for histopathological analyses. H&E and Masson's trichrome staining were performed using the commercial kits (DAKO) following standard procedures. For immunofluorescent staining, serial sections (10 μm) from OCT-embedded frozen tissues or primary cultured cells were fixed in cold acetone or 4% paraformaldehyde. After blocking with 1% goat serum, sections were incubated at room temperature with primary antibodies for 2 hours and then fluorescent dye-conjugated secondary antibodies for 1 hour. Images were acquired with a fluorescence microscopy (Nikon Instruments Inc).

Reverse transcription-PCR (RT-PCR) and quantitative PCR (qPCR)

Trizol reagent (Invitrogen) was used to extract total RNA following the manufacturer's instruction. cDNA was synthesized by the iScript cDNA synthesis kit (Bio-Rad). RT-PCR was performed on the Bio-Rad C1000 thermal cycler. qPCR was performed on the MX3000P qPCR machine using SYBR Green qPCR Mastermix (Agilent). The primers used were described previously (18).

Western blotting

PEMs, BMDMs, or skin and lung tissues were lysed in RIPA lysis buffer (1% Nonidet P-40, 0.1% sodium dodecyl sulfate (SDS), 0.5% sodium deoxycholate, 1 mM sodium orthovanadate, and protease inhibitors) to extract the total proteins. Samples were separated on SDS-polyacrylamide gels and electro-transferred onto nitrocellulose membranes (Amersham Biosciences). After blocking with 5% BSA, the membranes were incubated with various primary antibodies at 4 °C overnight. The membranes were then incubated with IRDye secondary antibodies (LI-COR Biosciences) at room temperature for 1 hour. The protein expression was detected by Odyssey CLx Imaging System (LI-COR Biosciences).

Co-immunoprecipitation (IP)

The protein A/G-agarose beads (Santa Cruz, CA) were incubated with IgG, RGC32 or NF-κB antibody at 4°C for 2 hours. BMDMs were lysed in 500 μl Co-IP lysis buffer (Pierce) on ice for 5 min. Following rapid centrifugation, the supernatants were incubated with beads at 4°C overnight. After washing with the Co-IP buffer, proteins were eluted from the beads and boiled in SDS loading buffer. Western blotting was performed to detect the precipitation of proteins.

Chromatin immunoprecipitation Assay (ChIP)

ChIP assays were performed using ChIP kit (Millipore) according to the manufacture's protocol. BMDMs were treated with IFNγ and LPS for 30 minutes. Chromatin complexes were immunoprecipitated with 3 ug of IgG (negative control), NF-κB or RGC32 antibodies. Semiquantitative PCR was performed to amplify the iNOS and IL-1β promoter regions containing the NF-κB binding site. The primers for iNOS promoter are 5'-AAA GGA GAA ACA GCC ACC AAG C-3' (forward) and 5'-AGC ACC CAC AAC CCA AAG AAC-3' (reverse). The primers for IL-1β promoter are 5'-TCC CTG GAA GTC AAG GGG TGG-3' (forward) and 5'-TCT GGG TGT GCA TCT ACG TGC C-3' (reverse).

Statistical analysis

All data are presented as the mean + SD. Student's unpaired t-test or 1-way ANOVA followed by the Fisher t test for comparison of means was used to compare groups. A P value less than 0.05 is considered to be statistically significant.

Results

RGC32 was essential for the development of SSc

Bleomycin-induced skin fibrosis in mice was used to study SSc (24). RGC32 expression was significantly up-regulated at both mRNA (Fig 1A) and protein (Fig 1B) levels in skin tissues along with SSc progression. Remarkably, a substantial increase of RGC32 expression was observed at the initial stage following one day of bleomycin injection (Fig 1A–1B), suggesting a role of RGC32 in SSc development.

One hallmark of skin fibrosis is the thickened dermis due to collagen deposition. Bleomycin caused a significant skin thickening 28 day after the injection, as measured by ultrasonic inspection. However, RGC32−/− diminished the skin thickening (Fig 1C and 1D). Histopathological analyses of the skin sections confirmed that the bleomycin-induced skin thickness in WT mice was significantly reduced in RGC32−/− mice (Fig 1E, left). Since fibrosis is characterized by excessive collagen deposition, we detected the collagen content using Masson's trichrome staining. Bleomycin induced a large amount of collagen deposition in the skin tissues of WT mice, but it was attenuated in RGC32−/− mice (Fig 1E, right). Consistently, the expression of collagen protein COL1A1 was also considerably decreased in bleomycin-treated RGC32−/− mice (Fig 1F).

The pulmonary lesion in patients with SSc is strongly associated with the mortality (25), thus we sought to determine if RGC32 plays a role in lung sclerosis. Lung fibrosis was induced by bleomycin in WT and RGC32−/− mice. Bleomycin treatment significantly impaired the lung structure as analyzed by H&E staining (Fig 1G). However, in RGC32−/− mice, the bleomycin-induced lung damage was remarkably alleviated (Fig 1G). Furthermore, bleomycin-treated RGC32−/− mice exhibited a marked reduction of collagen deposition and expression in the lung compared to WT mice (Fig 1G, right and 1H). These results further demonstrated that RGC32 played a critical role in the development of SSc.

RGC32 deficiency attenuated bleomycin-induced inflammation in skin tissues

Since RGC32 is abundantly expressed at the initial stage of SSc, it may regulate the early events of SSc. Macrophage infiltration is one of the essential factors initiating the SSc (26). In bleomycin-induced SSs, we observed a rapid presence of macrophages in skin, as evidenced by the elevation of macrophage marker F4/80 (Fig 2A). Notably, the highest F4/80 level was observed at day 1 after bleomycin injection, concomitant with the RGC32 expression (Fig 1A). We thus supposed that RGC32 was expressed in macrophages. Indeed, RGC32 was co-stained with F4/80 (Fig 2B) but not CD3 (Supplemental Fig 1A), indicating that RGC32 was mainly expressed in macrophages during the initiation phase of skin sclerosis. Moreover, RGC32−/− mice exhibited decreased macrophage infiltration in bleomycin-treated skin as shown by flow cytometry analysis (Fig 2C–2D), suggesting that RGC32 promoted bleomycin-induced SSc by modulating macrophage function.

Inflammation is known to be a critical factor driving the pathogenesis of SSc (27). We therefore investigated the inflammatory response in bleomycin-induced skin by analyzing the expression of major inflammatory mediator iNOS and IL-1β. Bleomycin treatment markedly increased the expression of both iNOS and IL-1β mRNAs (Supplemental Fig 1B) and proteins (Fig 2E–2G) in WT mouse skin tissues. Immunostaining of skin sections showed that both iNOS (Fig 2F) and IL-1β (Fig 2G) were co-localized with F4/80, indicating that these inflammatory mediators were mainly expressed by F4/80+ macrophages. Notably, bleomycin-treated RGC32−/− skin showed a lower inflammation, as evidenced by the attenuated expression of iNOS and IL-1β at both mRNA (Supplemental Fig 1B) and protein (Fig 2E) levels compared to WT skins. The reduced iNOS and IL-1β expression was concomitant with the less number of F4/80+ macrophages in RGC32−/− mouse skins (Fig 2F–2G).

In addition to inflammatory macrophages, alternatively activated macrophages (M2) were reported to also play an important role in perpetuating the Ssc (13). We therefore tested if RGC-32 affects M2 macrophage content in Ssc. Treatment with bleomycin for 28 days caused an accumulation of numerous arginase+ cells in WT mouse skins (Fig 2H), suggesting an increased M2 macrophage infiltration. However, RGC32−/− significantly attenuated the presence of arginase+ cells (Fig 2H). The reduction of arginase+ cells was concomitant with the decreased F4/80+ macrophages in RGC32−/− mouse skins further indicated that RGC-32 promoted the M2 infiltration (Fig 2H). The critical role of RGC-32 in arginase expression was also confirmed by Western blot analyses (Fig 2I), consistent with our previous studies showing that RGC-32 promotes M2 macrophage polarization in vitro (18). These results suggested that RGC32 regulated both the M1 and M2 macrophage function in the development of SSc.

Macrophage RGC32 was essential for SSc and the inflammation in bleomycin-treated skins

To determine if RGC32 in macrophage is essential for bleomycin-induced skin fibrosis, BMCs from either WT or RGC32−/− mice were adoptively transferred into lethally irradiated WT recipient mice to establish full bone marrow chimeras. 8 weeks after transfer, recipient mice were treated with bleomycin and skin fibrosis was assessed. Similar to WT mice, bleomycin treatment of recipient mice receiving WT BMCs caused intensive skin

sclerosis shown by the thickened dermis (Fig 3A, left) and exacerbated collagen deposition and expression (Fig 3A, right and 3B). However, recipient mice receiving RGC32−/− BMCs, in which the hematopoietic-derived cells were deficient in RGC32, exhibited significantly thinner skin (Fig 3A, left) and marked reduction in collagen deposition under bleomycin treatment (Fig 3A–3B). Moreover, recipient mice receiving RGC32−/− BMCs showed an alleviated inflammatory response in the skins after bleomycin treatment as the inflammatory mediator iNOS and IL-1β expression was significantly decreased compared to the recipients receiving WT BMCs (Fig 3C). These results indicated that macrophage RGC32-mediated inflammation is essential for the SSc development.

The function of macrophage RGC32 in lung impairment was also assessed in bleomycin-induced lung fibrosis in full bone marrow chimeras. The lung fibrosis induced by bleomycin in the recipient mice receiving RGC32−/− BMCs was significantly attenuated as compared to the recipients receiving WT BMCs, as shown by the improved lung morphology (Fig 3D, left) and the decreased collagen deposition (Fig 3D, right and 3E). These data demonstrated that RGC32 also promoted lung sclerosis via modulating macrophage function.

RGC32 was required for the polarization of classically activated macrophages

The observation that RGC32 in macrophage regulating inflammation in SSc led us to further study the role of RGC32 in inflammatory macrophage differentiation using PEMs and BMDMs. RGC32 was highly expressed in PEMs and M-CSF-induced BMDMs (Supplemental Fig 1C–1D). Importantly, RGC32 protein levels were significantly elevated in PEMs upon stimulation with IFNγ and LPS, well-known factors inducing the classically-activated macrophages (Fig 4A). Similar results were observed in IFNγ+LPS-treated BMDMs (Fig 4B).

To determine how RGC-32 is regulated in macrophages, pathway-specific inhibitors were used to identify signaling pathways that mediated the induction of RGC32 in classically activated macrophages. Inhibition of p38 mitogen-activated protein kinases (p38 MAPK) activity did not affect RGC32 mRNA or protein expression (Supplemental Fig 1E–1G) in BMDMs. However, blockade of the phosphatidylinositol-4,5-bisphosphate 3-kinase (PI3K), extracellular signal–regulated kinases (ERK), and c-Jun N-terminal kinase (JNK) significantly inhibited RGC32 expression (Supplemental Fig 1E–1G), suggesting that PI3K, ERK, and JNK signaling pathways regulated RGC32 expression in classically activated macrophages.

To determine if RGC32 is critical for the inflammatory function of classical activation of macrophages, we compared the iNOS and IL-1β expression in classically activated PEMs and BMDMs in WT and RGC32−/− mice. IFNγ and LPS stimulation induced a remarkable increase in iNOS and IL-1β protein expression in WT, but not RGC32−/− PEMs (Fig 4C–4D). Consistently, the iNOS and IL-1β expression was markedly decreased in RGC32−/− BMDMs compared to the WT with IFNγ and LPS stimulation (Fig 4E–4F). These results supported that RGC32 promoted the polarization of classically activated inflammatory macrophages to initiate the SSc.

RGC32 regulated M1 macrophages via the classical NF-κB pathway

Previous studies have shown that NF-κB activation promotes M1 macrophage polarization (28). We speculated that RGC32 activated M1 macrophage by modulating NF-κB signaling pathway and detected the phosphorylation of IκB and NF-κB (p65) in bleomycin-induced SSc. In agreement with the expression of iNOS and IL-1β (Fig 2E–2G), bleomycin significantly augmented the phosphorylation of both IκB and NF-κB in WT but not RGC32−/− skin (Fig 5A–5B).

The involvement of NF-κB signaling in RGC32-promoted classical activation of macrophages was assessed in PEMs and BMDMs stimulated with IFNγ+LPS. While the phosphorylation of IκB and NF-κB was induced by IFNγ+LPS in WT PEMs (Fig 5C–5D) and BMDMs (Fig 5E–5F), RGC32 deficiency markedly blocked the phosphorylation in both cells (Fig 5C–5F). Since NF-κB is sequestered in an inactive state in the cytoplasm by IκB, and translocated into the nuclei upon activation to regulate target gene expression (29), we compared the cytoplasmic and nuclear levels of NF-κB in WT and RGC32−/− BMDMs upon IFNγ+LPS induction. IFNγ+LPS-induced NF-κB nuclear translocation was significantly impaired in RGC32-deficient BMDMs, as evidenced by the lower level of nuclear NF-κB with relatively higher level of cytoplasmic NF-κB (Fig 5G–5I) as compared to the WT BMDMs. These data indicated that RGC32 regulated inflammatory response of macrophages at the early stage of SSc via the classical NF-κB signaling pathway.

RGC32 interacted with NF-κB and bound to the promoters of inflammatory mediators

In macrophages, NF-κB activates iNOS and IL-1β expression by direct binding to their promoters as a transcriptional factor (30, 31). Therefore, RGC32 may regulate iNOS and IL-1β expression in M1 macrophages by cooperation with NF-κB. Co-IP assays were performed to test the direct interaction between endogenous RGC32 and NF-κB in macrophages. In classically activated WT BMDMs, NF-κB was pulled down along with RGC32 (Fig 6A–6B) and vice versa (Fig 6C–6D), indicating a strong interaction between RGC32 and NF-κB in M1 macrophages. The interaction of RGC32 and NF-κB was minimal in undifferentiated BMDM.

Since RGC32 interacted with NF-κB, and they are both critical in the mRNA expression of inflammatory mediators iNOS and IL-1β (30, 31) (Supplemental Fig 1B), we performed ChIP assays to test if RGC32 binds to the NF-κB binding regions in iNOS and IL-1β promoters. As shown in Fig 6E–6F, RGC32 indeed bound to the same promoter regions of iNOS and IL-1β as NF-κB. Due to the lack of a DNA binding domain, we tested if NF-κB is required for RGC32 binding to iNOS and IL-1β promoters. Blockade of NF-κB nuclear translocation by ammonium pyrrolidine dithiocarbamate (PDTC) diminished RGC32 binding to the promoters and inhibited RGC32-enhanced iNOS and IL-1β expression in macrophages (Fig 6G–6H), demonstrating that RGC32 promoted the inflammation response in classically activated macrophages through NF-κB signaling.

Discussion

SSc is a chronic autoimmune disorder characterized by diffuse fibrosis in the skin, joints and internal organs (such as lungs and kidneys) (32, 33). It is widely accepted that the vascular endothelial activation and excessive deposition of extracellular matrix in SSs are highly associated with the inflammatory abnormalities (34). Previous studies show that RGC32 is involved in renal fibrosis by mediating fibroblast activation (20). By using RGC32−/− mice, we found that RGC32 deficiency significantly ameliorated the bleomycin-induced skin and lung sclerosis, as evidenced by the reduction in dermis thickness and collagen deposition, demonstrating that RGC32 is an essential mediator for the SSc. Since the remarkable expression of RGC32 is induced at the very early stage of SSc, the major function of RGC32 in the onset of SSc is likely to be independent of fibroblasts that are activated and functioned in the late stage of SSc (35, 36).

Macrophages and T cells are involved in the onset of SSc (37–42). Macrophage accumulation was revealed at the early stage of bleomycin-induced skin sclerosis. RGC32 was abundantly expressed in macrophages, but not in T cells, during the early stage. RGC32 appeared to play an essential role in inducing macrophage infiltration and the inflammatory response of skin fibrosis as RGC32 deficiency reduced macrophage accumulation and markedly diminished the expression of two potent fibrosis inducers iNOS and IL-1β in skin tissues (43–46). The importance of macrophage RGC32 in SSc was also supported by the outcome of full bone marrow chimeric mice in which RGC32 deficiency in hematopoietic macrophages attenuated the skin and lung sclerosis.

RGC32 regulated the pro-inflammatory response of M1 macrophages. IFNγ and LPS stimulation of PEMs and BMDMs induced RGC32 expression through PI3K, ERK, and JNK signaling pathways. RGC32 deficiency significantly impaired IFNγ and LPS-stimulated elevation of iNOS and IL-1β in both PEMs and BMDMs. A previous report showed that LPS decreased RGC32 mRNA expression in macrophages (19). The discrepancy is likely due to the different treatment times. In the previous report, macrophages were treated with IFNγ and LPS for 42 hours, which might cause a negative feedback mechanism, resulting in a reduction in RGC32 mRNA level. Our results clearly showed that increased expression of RGC32 was critical for the polarization and inflammatory response of classically activated macrophages.

RGC32 interacted with NF-κB signaling to mediate M1 macrophage polarization (9, 10, 47) and skin fibrosis (48–51). The activation of NF-κB signaling was significantly inhibited in bleomycin-treated RGC32−/− skin tissues as well as in IFNγ and LPS-treated RGC32−/− PEMs and BMDMs. On the other hand, RGC32 promoted iNOS and IL-1β expression in a NF-κB-dependent manner as blockade of NF-κB nuclear translocation diminished RGC32-mediated iNOS and IL-1β expression. It appeared that RGC32 regulated iNOS and IL-1β expression by binding to their promoters (30, 31) through interacting with NF-κB.

Our previous studies showed that RGC32 deficiency inhibited IL-4-stimulated canonical M2 macrophage to express arginase (18). The arginase expression was increased in WT mouse skin tissues, but was attenuated in RGC32−/− skin, suggesting that RGC32 was also

important for the polarization of alternative activated macrophages in the development of Ssc. Thus, the marked reduction of skin fibrosis in RGC32−/− mice was likely due to both the impaired M1 macrophage function at the early stage and the impaired M2 macrophage function at the late stage of skin sclerosis.

Taken together, our studies revealed a crucial role of RGC32 in the onset of SSc in both skin and lung fibrosis. RGC32 promoted classically activated macrophage polarization and regulated the expression of inflammatory mediators through directly interacting with NF-κB. Therefore, targeting RGC32 serves a novel therapeutic strategy in treating sclerosis disease.

Supplementary Material

Refer to Web version on PubMed Central for supplementary material.

Acknowledgments

We thank Dr. Wendy Watford for her technical assistance in bone marrow transplantation experiments.

References

1. Asano Y. Future treatments in systemic sclerosis. J Dermatol. 2010; 37:54–70. [PubMed: 20175840]
2. Almeida I, Faria R, Vita P, Vasconcelos C. Systemic sclerosis refractory disease: from the skin to the heart. Autoimmun Rev. 2011; 10:693–701. [PubMed: 21575745]
3. Taniguchi T, Asano Y, Akamata K, Noda S, Takahashi T, Ichimura Y, Toyama T, Trojanowska M, Sato S. Fibrosis, vascular activation, and immune abnormalities resembling systemic sclerosis in bleomycin-treated Fli-1-haploinsufficient mice. Arthritis Rheumatol. 2015; 67:517–526. [PubMed: 25385187]
4. Bhattacharyya S, Wei J, Varga J. Understanding fibrosis in systemic sclerosis: shifting paradigms, emerging opportunities. Nat Rev Rheumatol. 2011; 8:42–54. [PubMed: 22025123]
5. Lakos G, Melichian D, Wu M, Varga J. Increased bleomycin-induced skin fibrosis in mice lacking the Th1-specific transcription factor T-bet. Pathobiology. 2006; 73:224–237. [PubMed: 17314493]
6. Yamamoto T, Nishioka K. Animal model of sclerotic skin. VI: Evaluation of bleomycin-induced skin sclerosis in nude mice. Arch Dermatol Res. 2004; 295:453–456. [PubMed: 14673598]
7. Helene M, Lake-Bullock V, Zhu J, Hao H, Cohen DA, Kaplan AM. T cell independence of bleomycin-induced pulmonary fibrosis. J Leukoc Biol. 1999; 65:187–195. [PubMed: 10088601]
8. Mosser DM, Edwards JP. Exploring the full spectrum of macrophage activation. Nat Rev Immunol. 2008; 8:958–969. [PubMed: 19029990]
9. Rius J, Guma M, Schachtrup C, Akassoglou K, Zinkernagel AS, Nizet V, Johnson RS, Haddad GG, Karin M. NF-kappaB links innate immunity to the hypoxic response through transcriptional regulation of HIF-1alpha. Nature. 2008; 453:807–811. [PubMed: 18432192]
10. Wu XQ, Yang Y, Li WX, Cheng YH, Li XF, Huang C, Meng XM, Wu BM, Liu XH, Zhang L, Lv XW, Li J. Telomerase reverse transcriptase acts in a feedback loop with NF-kappaB pathway to regulate macrophage polarization in alcoholic liver disease. Sci Rep. 2016; 6:18685. [PubMed: 26725521]
11. Hussein MR, Hassan HI, Hofny ER, Elkholy M, Fatehy NA, Abd Elmoniem AE, Ezz El-Din AM, Afifi OA, Rashed HG. Alterations of mononuclear inflammatory cells, CD4/CD8+ T cells, interleukin 1beta, and tumour necrosis factor alpha in the bronchoalveolar lavage fluid, peripheral blood, and skin of patients with systemic sclerosis. J Clin Pathol. 2005; 58:178–184. [PubMed: 15677539]

12. Becker H, Stengl G, Stein M, Federlin K. Analysis of proteins that interact with the IL-2 regulatory region in patients with rheumatic diseases. Clin Exp Immunol. 1995; 99:325–330. [PubMed: 7882553]
13. Stifano G, Christmann RB. Macrophage Involvement in Systemic Sclerosis: Do We Need More Evidence? Curr Rheumatol Rep. 2016; 18:2. [PubMed: 26700912]
14. Higashi-Kuwata N, Jinnin M, Makino T, Fukushima S, Inoue Y, Muchemwa FC, Yonemura Y, Komohara Y, Takeya M, Mitsuya H, Ihn H. Characterization of monocyte/macrophage subsets in the skin and peripheral blood derived from patients with systemic sclerosis. Arthritis Res Ther. 2010; 12:R128. [PubMed: 20602758]
15. Schlick SN, Wood CD, Gunnell A, Webb HM, Khasnis S, Schepers A, West MJ. Upregulation of the cell-cycle regulator RGC-32 in Epstein-Barr virus-immortalized cells. PLoS One. 2011; 6:e28638. [PubMed: 22163048]
16. Huang WY, Li ZG, Rus H, Wang X, Jose PA, Chen SY. RGC-32 mediates transforming growth factor-beta-induced epithelial-mesenchymal transition in human renal proximal tubular cells. J Biol Chem. 2009; 284:9426–9432. [PubMed: 19158077]
17. Wang JN, Shi N, Xie WB, Guo X, Chen SY. Response gene to complement 32 promotes vascular lesion formation through stimulation of smooth muscle cell proliferation and migration. Arterioscler Thromb Vasc Biol. 2011; 31:e19–26. [PubMed: 21636805]
18. Tang R, Zhang G, Chen SY. Response gene to complement 32 protein promotes macrophage phagocytosis via activation of protein kinase C pathway. J Biol Chem. 2014; 289:22715–22722. [PubMed: 24973210]
19. Zhao P, Gao D, Wang Q, Song B, Shao Q, Sun J, Ji C, Li X, Li P, Qu X. Response gene to complement 32 (RGC-32) expression on M2-polarized and tumor-associated macrophages is M-CSF-dependent and enhanced by tumor-derived IL-4. Cell Mol Immunol. 2015; 12:692–699. [PubMed: 25418473]
20. Li Z, Xie WB, Escano CS, Asico LD, Xie Q, Jose PA, Chen SY. Response gene to complement 32 is essential for fibroblast activation in renal fibrosis. J Biol Chem. 2011; 286:41323–41330. [PubMed: 21990365]
21. Cui XB, Guo X, Chen SY. Response gene to complement 32 deficiency causes impaired placental angiogenesis in mice. Cardiovasc Res. 2013; 99:632–639. [PubMed: 23695833]
22. Sun C, Sun L, Ma H, Peng J, Zhen Y, Duan K, Liu G, Ding W, Zhao Y. The phenotype and functional alterations of macrophages in mice with hyperglycemia for long term. J Cell Physiol. 2012; 227:1670–1679. [PubMed: 21678423]
23. Sun L, Sun C, Liang Z, Li H, Chen L, Luo H, Zhang H, Ding P, Sun X, Qin Z, Zhao Y. FSP1(+) fibroblast subpopulation is essential for the maintenance and regeneration of medullary thymic epithelial cells. Sci Rep. 2015; 5:14871. [PubMed: 26445893]
24. Avouac J, Elhai M, Allanore Y. Experimental models of dermal fibrosis and systemic sclerosis. Joint Bone Spine. 2013; 80:23–28. [PubMed: 22841579]
25. Morales-Cardenas A, Perez-Madrid C, Arias L, Ojeda P, Mahecha MP, Rojas-Villarraga A, Carrillo-Bayona JA, Anaya JM. Pulmonary involvement in systemic sclerosis. Autoimmun Rev. 2016; 15:1094–1108. [PubMed: 27497912]
26. York MR, Nagai T, Mangini AJ, Lemaire R, van Seventer JM, Lafyatis R. A macrophage marker, Siglec-1, is increased on circulating monocytes in patients with systemic sclerosis and induced by type I interferons and toll-like receptor agonists. Arthritis Rheum. 2007; 56:1010–1020. [PubMed: 17328080]
27. Barnes TC, Anderson ME, Moots RJ. The many faces of interleukin-6: the role of IL-6 in inflammation, vasculopathy, and fibrosis in systemic sclerosis. Int J Rheumatol. 2011; 2011:721608. [PubMed: 21941555]
28. Hou Y, Lin H, Zhu L, Liu Z, Hu F, Shi J, Yang T, Shi X, Zhu M, Godley BF, Wang Q, Li Z, Zhao Y. Lipopolysaccharide increases the incidence of collagen-induced arthritis in mice through induction of protease HTRA-1 expression. Arthritis Rheum. 2013; 65:2835–2846. [PubMed: 23982886]
29. Perkins ND. Integrating cell-signalling pathways with NF-kappaB and IKK function. Nat Rev Mol Cell Biol. 2007; 8:49–62. [PubMed: 17183360]

30. Simon PS, Sharman SK, Lu C, Yang D, Paschall AV, Tulachan SS, Liu K. The NF-kappaB p65 and p50 homodimer cooperate with IRF8 to activate iNOS transcription. BMC Cancer. 2015; 15:770. [PubMed: 26497740]

31. Scheibel M, Klein B, Merkle H, Schulz M, Fritsch R, Greten FR, Arkan MC, Schneider G, Schmid RM. IkappaBbeta is an essential co-activator for LPS-induced IL-1beta transcription in vivo. J Exp Med. 2010; 207:2621–2630. [PubMed: 20975042]

32. Bournia VK, Vlachoyiannopoulos PG, Selmi C, Moutsopoulos HM, Gershwin ME. Recent advances in the treatment of systemic sclerosis. Clin Rev Allergy Immunol. 2009; 36:176–200. [PubMed: 19132559]

33. Lefevre G, Dauchet L, Hachulla E, Montani D, Sobanski V, Lambert M, Hatron PY, Humbert M, Launay D. Survival and prognostic factors in systemic sclerosis-associated pulmonary hypertension: a systematic review and meta-analysis. Arthritis Rheum. 2013; 65:2412–2423. [PubMed: 23740572]

34. Shanmugam VK, Swistowski DR, Saddic N, Wang H, Steen VD. Comparison of indirect immunofluorescence and multiplex antinuclear antibody screening in systemic sclerosis. Clin Rheumatol. 2011; 30:1363–1368. [PubMed: 21614475]

35. Zhang HY, Gharaee-Kermani M, Zhang K, Karmiol S, Phan SH. Lung fibroblast alpha-smooth muscle actin expression and contractile phenotype in bleomycin-induced pulmonary fibrosis. Am J Pathol. 1996; 148:527–537. [PubMed: 8579115]

36. Phan SH. The myofibroblast in pulmonary fibrosis. Chest. 2002; 122:286S–289S. [PubMed: 12475801]

37. Liu M, Yang J, Xing X, Cui X, Li M. Interleukin-17A promotes functional activation of systemic sclerosis patient-derived dermal vascular smooth muscle cells by extracellular-regulated protein kinases signalling pathway. Arthritis Res Ther. 2014; 16:4223. [PubMed: 25551434]

38. Slobodin G, Ahmad MS, Rosner I, Peri R, Rozenbaum M, Kessel A, Toubi E, Odeh M. Regulatory T cells (CD4(+)CD25(bright)FoxP3(+)) expansion in systemic sclerosis correlates with disease activity and severity. Cell Immunol. 2010; 261:77–80. [PubMed: 20096404]

39. Ayano M, Tsukamoto H, Kohno K, Ueda N, Tanaka A, Mitoma H, Akahoshi M, Arinobu Y, Niiro H, Horiuchi T, Akashi K. Increased CD226 Expression on CD8+ T Cells Is Associated with Upregulated Cytokine Production and Endothelial Cell Injury in Patients with Systemic Sclerosis. J Immunol. 2015; 195:892–900. [PubMed: 26109642]

40. Christmann RB, Lafyatis R. The cytokine language of monocytes and macrophages in systemic sclerosis. Arthritis Res Ther. 2010; 12:146. [PubMed: 21067557]

41. Failli P, Palmieri L, D'Alfonso C, Giovannelli L, Generini S, Rosso AD, Pignone A, Stanflin N, Orsi S, Zilletti L, Matucci-Cerinic M. Effect of N-acetyl-L-cysteine on peroxynitrite and superoxide anion production of lung alveolar macrophages in systemic sclerosis. Nitric Oxide. 2002; 7:277–282. [PubMed: 12446176]

42. Andersen GN, Nilsson K, Nagaeva O, Rantapaa-Dahlqvist S, Sandstrom T, Mincheva-Nilsson L. Cytokine mRNA profile of alveolar T lymphocytes and macrophages in patients with systemic sclerosis suggests a local Tr1 response. Scand J Immunol. 2011; 74:272–281. [PubMed: 21535076]

43. Zhang JD, Patel MB, Griffiths R, Dolber PC, Ruiz P, Sparks MA, Stegbauer J, Jin H, Gomez JA, Buckley AF, Lefler WS, Chen D, Crowley SD. Type 1 angiotensin receptors on macrophages ameliorate IL-1 receptor-mediated kidney fibrosis. J Clin Invest. 2014; 124:2198–2203. [PubMed: 24743144]

44. Iannitti RG, Napolioni V, Oikonomou V, De Luca A, Galosi C, Pariano M, Massi-Benedetti C, Borghi M, Puccetti M, Lucidi V, Colombo C, Fiscarelli E, Lass-Florl C, Majo F, Cariani L, Russo M, Porcaro L, Ricciotti G, Ellemunter H, Ratclif L, De Benedictis FM, Talesa VN, Dinarello CA, van de Veerdonk FL, Romani L. IL-1 receptor antagonist ameliorates inflammasome-dependent inflammation in murine and human cystic fibrosis. Nat Commun. 2016; 7:10791. [PubMed: 26972847]

45. Gordon S. Alternative activation of macrophages. Nat Rev Immunol. 2003; 3:23–35. [PubMed: 12511873]

46. Takagi K, Kawaguchi Y, Hara M, Sugiura T, Harigai M, Kamatani N. Serum nitric oxide (NO) levels in systemic sclerosis patients: correlation between NO levels and clinical features. Clin Exp Immunol. 2003; 134:538–544. [PubMed: 14632763]

47. Wang N, Liang H, Zen K. Molecular mechanisms that influence the macrophage m1–m2 polarization balance. Front Immunol. 2014; 5:614. [PubMed: 25506346]

48. Bell S, Degitz K, Quirling M, Jilg N, Page S, Brand K. Involvement of NF-kappaB signalling in skin physiology and disease. Cell Signal. 2003; 15:1–7. [PubMed: 12401514]

49. Fullard N, Moles A, O'Reilly S, van Laar JM, Faini D, Diboll J, Reynolds NJ, Mann DA, Reichelt J, Oakley F. The c-Rel subunit of NF-kappaB regulates epidermal homeostasis and promotes skin fibrosis in mice. Am J Pathol. 2013; 182:2109–2120. [PubMed: 23562440]

50. O'Reilly S, Cant R, Ciechomska M, Finnigan J, Oakley F, Hambleton S, van Laar JM. Serum amyloid A induces interleukin-6 in dermal fibroblasts via Toll-like receptor 2, interleukin-1 receptor-associated kinase 4 and nuclear factor-kappaB. Immunology. 2014; 143:331–340. [PubMed: 24476318]

51. Arismendi M, Giraud M, Ruzehaji N, Dieude P, Koumakis E, Ruiz B, Airo P, Cusi D, Matucci-Cerinic M, Salvi E, Cuomo G, Hachulla E, Diot E, Caramaschi P, Riccieri V, Avouac J, Kayser C, Allanore Y. Identification of NF-kappaB and PLCL2 as new susceptibility genes and highlights on a potential role of IRF8 through interferon signature modulation in systemic sclerosis. Arthritis Res Ther. 2015; 17:71. [PubMed: 25880423]

Nonstandard abbreviations

RGC32	response gene to complement 32
Ssc	systemic sclerosis
PEM	peritoneal macrophages
BMDM	bone marrow derived macrophages
COL1A1	Collagen type I alpha 1
IP	immunoprecipitation
ChIP	chromatin immunoprecipitation

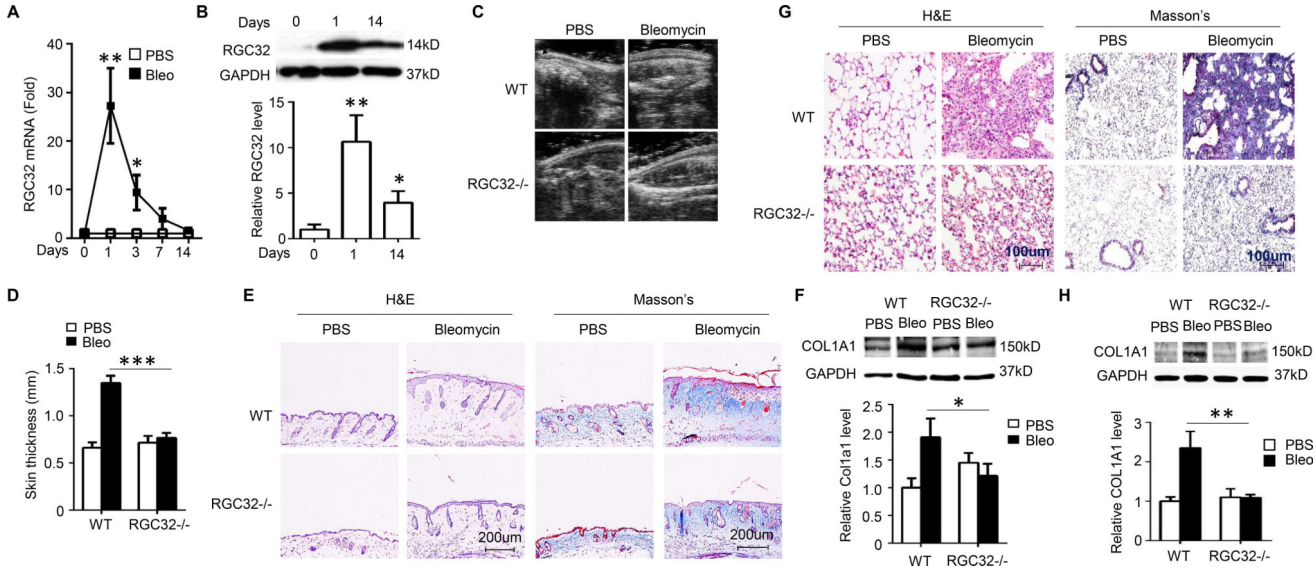

Figure 1. RGC32 deficiency ameliorated bleomycin-induced skin and lung fibrosis

(A–B) Mice were injected with bleomycin (Bleo, 0.02U) subcutaneously for the times indicated. RGC32 mRNA (A) and protein (B) expression during the early stage of skin fibrosis were detected by qPCR (A) and Western blotting (B), respectively. RGC32 protein levels in B were quantified by normalizing to GAPDH. *P<0.05, **P<0.01 compared to the control (PBS-treated or day 0, n=6). (C) RGC32 deletion (RGC32−/−) blocked bleomycin-induced skin fibrosis as compared to wild type mice (WT). Skin sections were collected 28 days after bleomycin injection. The skin thickness was measured by ultrasonic inspection. (D) Quantification of the skin thickness in bleomycin-treated WT and RGC32−/− mice compared to PBS control. **P < 0.01 (n=6). (E) RGC32−/− inhibited bleomycin-induced collagen deposition in skin as shown by Masson's trichrome staining. H&E staining showed skin structure. (F) RGC32−/− blocked bleomycin-induced Collagen I (COL1A1) expression in skin tissues as determined by Western blotting. COL1A1 protein levels were quantified by normalizing to GAPDH. *P < 0.05, n=6. (G–H) RGC32−/− blocked bleomycin-induced lung fibrosis. Lung fibrosis was induced in WT and RGC32−/− mice by bleomycin injection (0.2U) for 24 days. RGC32−/− inhibited bleomycin-induced collagen deposition in lung as shown by Masson's trichrome staining. H&E staining showed the lung structure (G). (H) RGC32−/− blocked bleomycin-induced COL1A1 expression in lung tissues as determined by Western blotting. COL1A1 protein levels were quantified by normalizing to GAPDH. **P < 0.01, n=6.

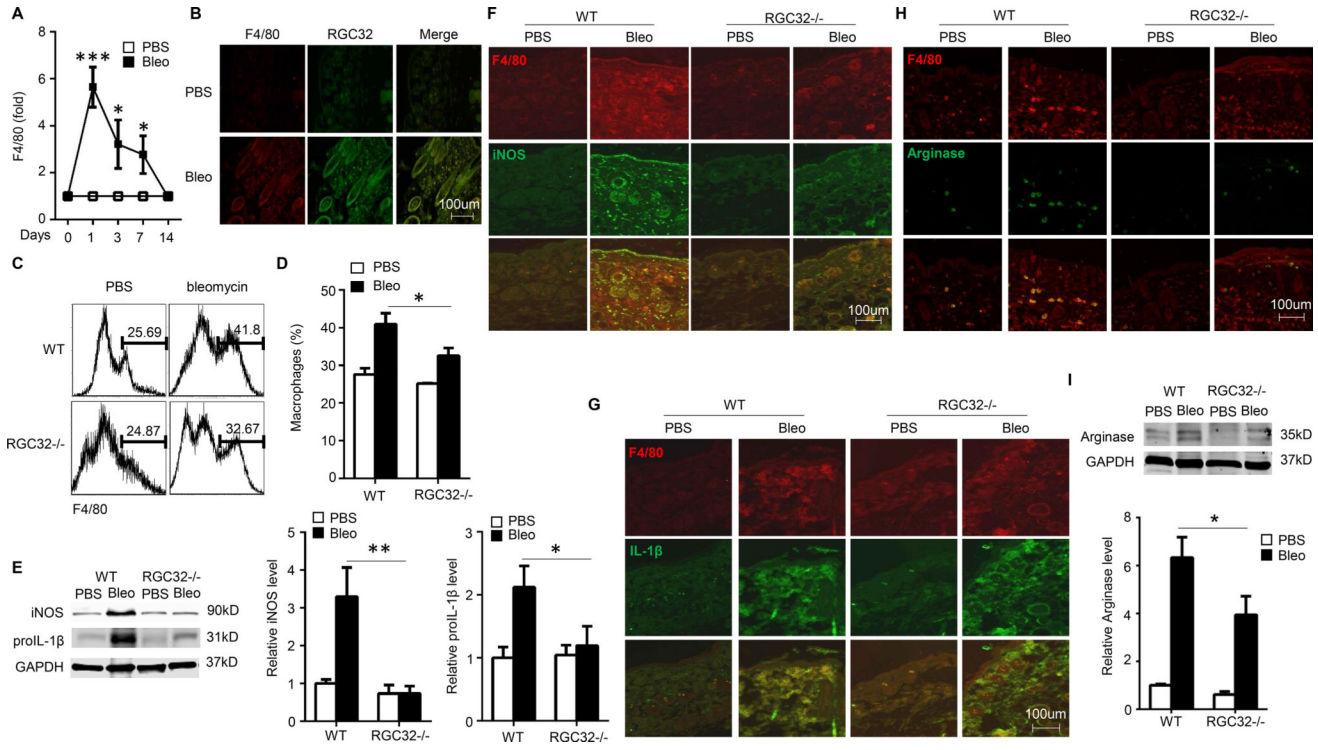

Figure 2. Macrophage RGC32 modulated the inflammation in bleomycin-induced skin sclerosis

Mice were injected with bleomycin (Bleo, 0.02U) subcutaneously for 0–14 days (A) or one day (B–G). (A) F4/80 mRNA expression was induced during the initial stage of skin fibrosis as detected by qPCR. *P<0.05, ***P<0.001 compared to PBS-treated skin tissues at the corresponding time points (n=6). (B) RGC32 was induced in F4/80-positive macrophages in the bleomycin-treated skin. Frozen sections of skin tissues were co-immunostained with F4/80 and RGC32 antibodies. (C–D) RGC32 deficiency (RGC32−/−) inhibited bleomycin-induced accumulation of F4/80+ macrophages in skin tissues. The percentage of F4/80+ macrophages was measured by flow cytometry. Shown are representative FACS analyses (C) and the percentage of F4/80+ macrophages (D) in PBS- or bleomycin-treated skins of wild type (WT) and RGC32−/− mice, *P<0.05, n=6. (E) RGC32−/− attenuated bleomycin-induced iNOS and IL-1β protein expression in mouse skins, as detected by Western blot. The protein levels of iNOS and proIL-1β were quantified by normalizing to GAPDH. *P<0.05, **P<0.01, n=6. (F–G) RGC32−/− attenuated bleomycin-induced iNOS and IL-1β expression in macrophages as co-immunostained with F4/80 and iNOS antibodies (F), or F4/80 and IL-1β antibodies in skin frozen sections (G). (H) RGC32−/− attenuated bleomycin-induced arginase expression in macrophages. Frozen skin sections were co-immunostained with F4/80 and arginase antibodies. (I) RGC32−/− attenuated bleomycin-induced arginase protein expression in mouse skins, as detected by Western blot. The protein levels of arginase were quantified by normalizing to GAPDH. *P < 0.05, n=6.

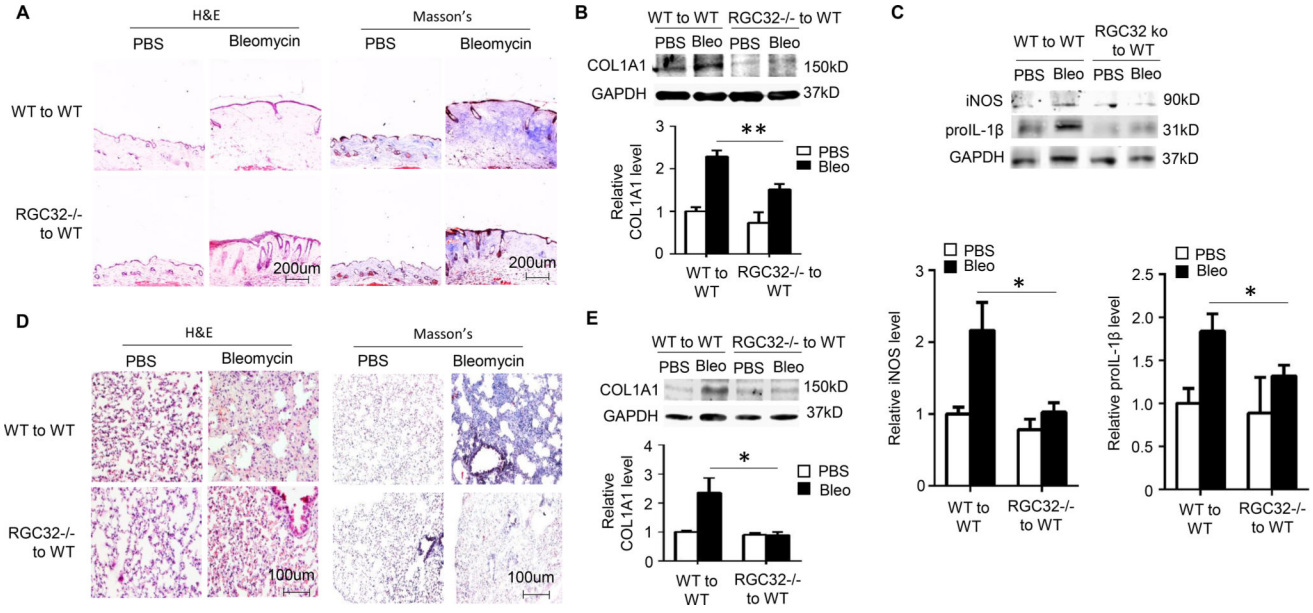

Figure 3. Macrophage RGC32 is required for skin and lung sclerosis development

(A–B) Full chimeric mice were generated by transplanting either WT or RGC32−/− BMCs to lethally irradiated WT mice. 8 weeks after the transplantation, recipient mice were treated with PBS or 0.02U bleomycin for 28 days to induce skin fibrosis. (A) Recipient mice receiving RGC32−/− BMCs exhibited a significant reduction in bleomycin-induced collagen deposition in skins compared to mice receiving WT BMCs as shown by Masson's trichrome staining. H&E staining indicated the skin structure. (B) Recipient mice received RGC32−/− BMCs showed a significant decrease in bleomycin-induced collagen I (COL1A1) expression in skin tissues as determined by Western blotting. COL1A1 protein levels were quantified by normalizing to GAPDH. **P<0.01, n=3. (C) The expression of iNOS and IL-1β was decreased in bleomycin-treated recipient mice receiving RGC32−/− BMCs compared to those receiving WT BMCs. The skin tissues were collected 1 day after bleomycin injection. The iNOS and proIL-1β protein expression were detected by Western blot and quantified by normalizing to GAPDH. *P < 0.05, n=6. (D–E) Full chimeric mice were generated similarly as described in A–B. 8 weeks after the transplantation, recipient mice were treated with PBS or 0.2U bleomycin for 24 days to induce lung fibrosis. (D) RGC32 deficient BMCs attenuated bleomycin-induced lung fibrosis as shown by the improved structure (H&E staining) and the reduced collagen deposition (Masson's trichrome staining). (E) COL1A11 protein expression in bleomycin-treated lung tissues was determined by Western blot. COL1A1 levels were quantified by normalizing to GAPDH. *P<0.05, n=6.

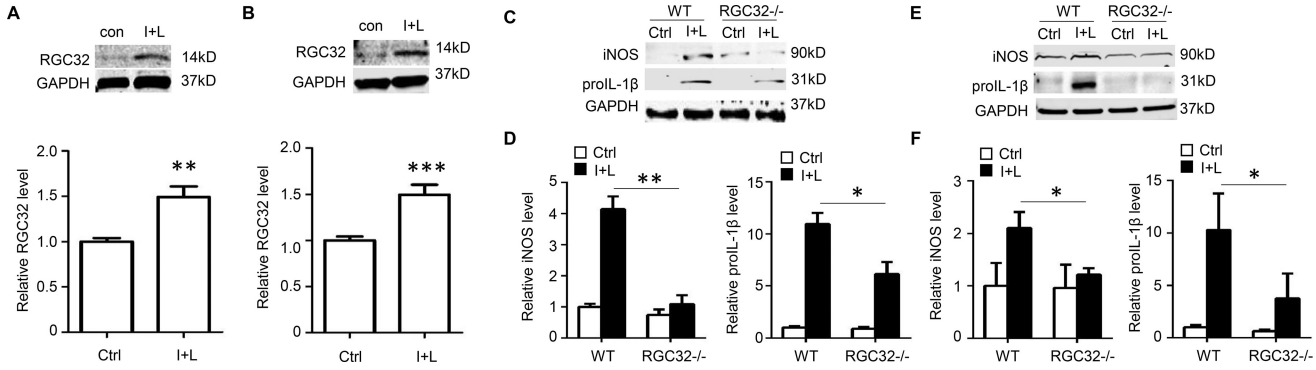

Figure 4. RGC32 mediated macrophage classical activation

(A–B) RGC32 was induced with IFNγ (100 ng/mL) and LPS (100 ng/mL) (I+L) in cultured PEMs and BMDMs. RGC32 protein levels in I+L-treated PEMs (A) and BMDMs (B) were measured by Western blot and quantified by normalizing to GAPDH, respectively. **P < 0.01, ***P < 0.001 compared with vehicle-treated cells (Ctrl), n=4. (C–F) RGC32 deficiency (RGC32−/−) inhibited I+L-induced iNOS and IL-1β production. PEMs (C–D) or BMDMs (E–F) isolated from WT or RGC32−/− mice were treated with vehicle (Ctrl) or I+L (100 ng/mL each) to induce macrophage classical activation. The expression of iNOS and IL-1β were determined by Western blot and quantified by normalizing to GAPDH, respectively. *P < 0.05, **P < 0.01, n=5.

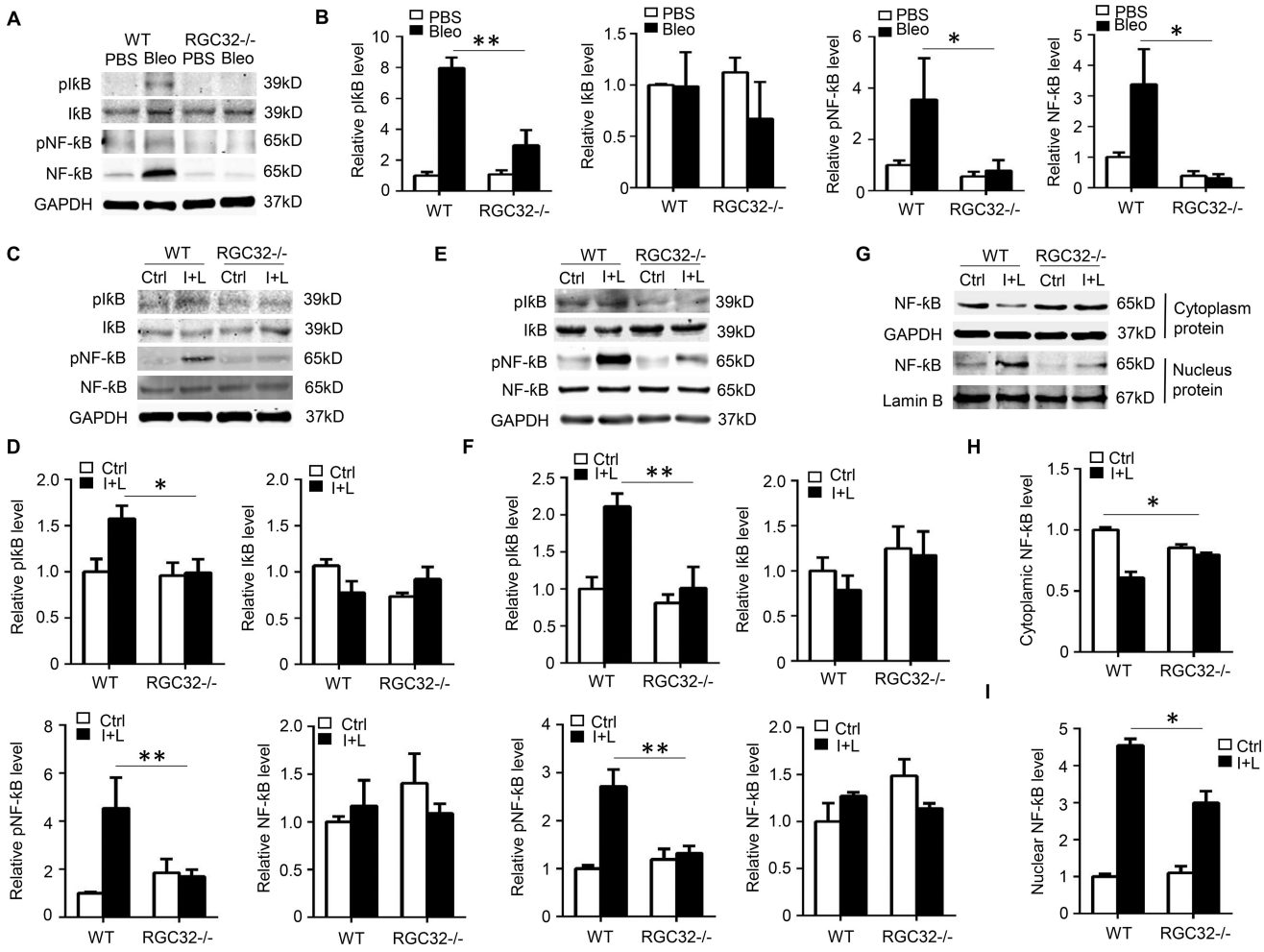

Figure 5. RGC32 was essential for the activation of NF-κB pathway in classically activated macrophages

(A–B) RGC32 deficiency (RGC32−/−) blocked of IκB (pIκB) and NF-κB (pNF-κB) phosphorylation in skin tissues. WT and RGC32−/− mice were injected with bleomycin (Bleo, 0.02U) subcutaneously. Skin tissues were collected 1 day after the bleomycin treatment. The expression of pIκB, IκB, pNF-κB and NF-κB was measured by Western blotting (A) and quantified by normalizing to GAPDH (B). *P<0.05, **P<0.01, n=6. (C–F) RGC32−/− significantly inhibited IFNγ+LPS (I+L)-induced increase in pIκB and pNF-κB levels in macrophages. PEMs (C, D) or BMDMs (E, F) isolated from WT and RGC32−/− mice were treated with 100 ng/mL IFNγ and 100 ng/mL LPS for 30 min. IκB, NF-κB, pIκB, and pNF-κB levels in PEMs (C) and BMDMs (E) were detected by Western blot and quantified by normalized to GAPDH (D–F), respectively. *P<0.05, **P<0.01, n=6. (G–I) RGC32−/− blocked I+I-induced NF-κB nuclear translocation. BMDMs isolated from WT and RGC32−/− mice were treated with 100 ng/mL IFNγ and 100 ng/mL LPS for 30 min. Cytoplasmic and nuclear protein fractions were prepared to detect the NF-κB distribution by Western blot (G). Cytoplasmic NF-κB level was quantified by normalizing to GAPDH (H), and nuclear NF-κB level was quantified by normalizing to Lamin B (I). *P < 0.05, n=4.

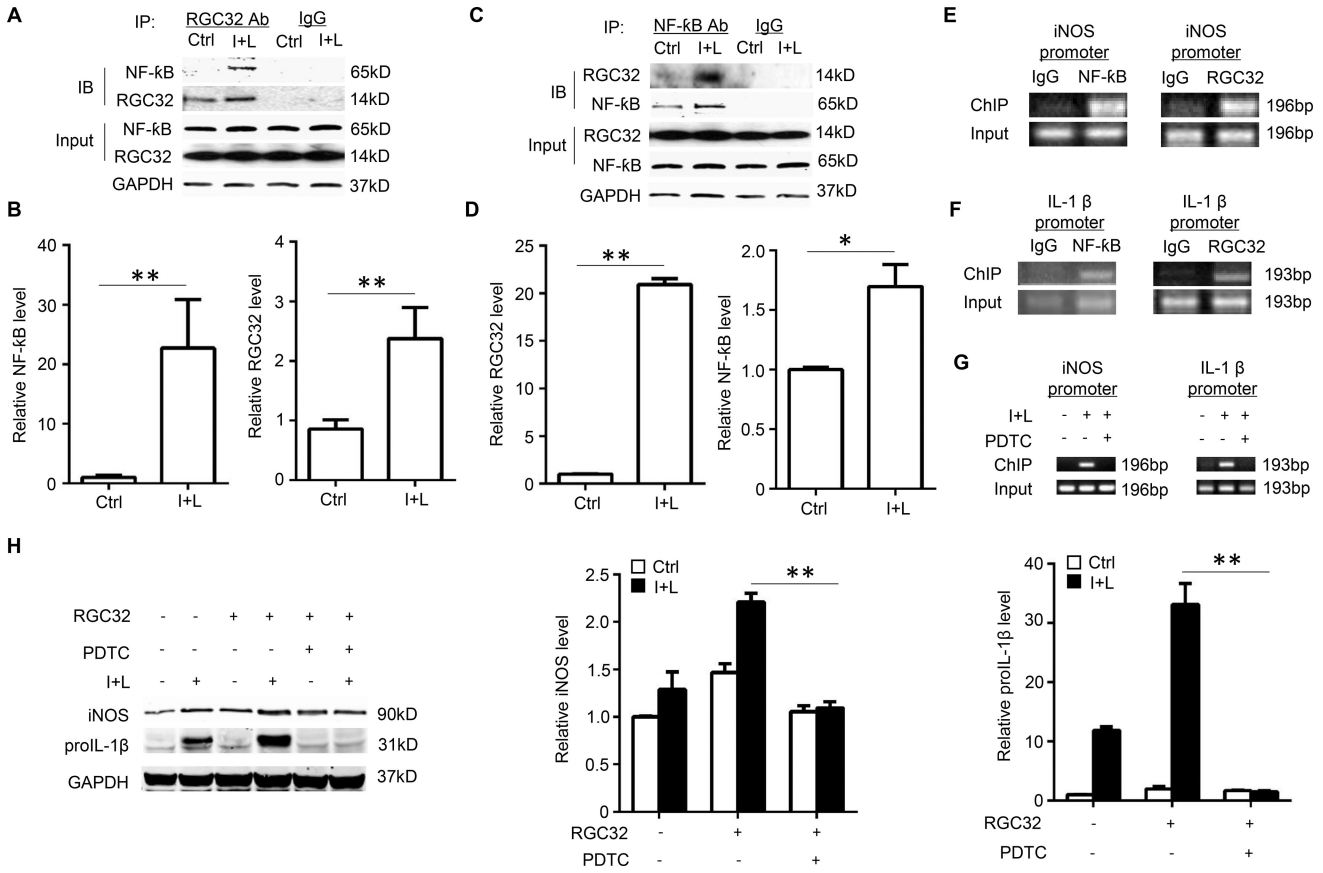

Figure 6. RGC32 interacted with NF-κB and bound to inflammatory gene promoters in classically activated macrophages

(A–D) NF-κB co-immunoprecipitated with RGC32 in classically activated macrophages. BMDMs from WT mice were stimulated with 100 ng/mL IFNγ and 100 ng/mL LPS for 6 h. Normal IgG isotype or antibodies against RGC32 (A) or NF-κB (C) were used for immunoprecipitation (IP). NF-κB (A) or RGC32 antibody (C) was used for immunoblotting (IB). (B, D) Quantification of NF-κB and RGC32 levels shown in (A) and (C) by normalizing to GAPDH, respectively. (E, F) RGC32 and NF-κB bound to the same regions of iNOS or IL-1β promoters. BMDMs were treated with 100 ng/mL IFNγ and 100 ng/mL LPS for 30 min followed by chromatin immunoprecipitation assay (ChIP) using control IgG, NF-κB, or RGC32 antibodies. PCR was performed to detect the RGC32 and NF-κB binding regions in iNOS (E) and IL-1β (F) promoters. (G) Blockade of NF-κB activation diminished RGC32 binding to the iNOS and IL-1β promoters in BMDMs. BMDMs were treated with 200 μM ammonium pyrrolidine dithiocarbamate (PDTC) for 1 hour, followed by treatment with 100 ng/mL IFNγ and 100 ng/mL LPS for 30 min. RGC32 antibodies were used for ChIP. PCR was performed to detect RGC32 binding to NF-κB binding regions in iNOS and IL-1β promoters. (H) Blockade of NF-κB activation inhibited RGC32-enhanced iNOS and IL-1β expression in RAW264.7 cells. RAW264.7 were transfected with control (−) or RGC32 expression plasmid. 24 h later, cells were treated with 200 μM PDTC for 1 hour followed by induction with 100 ng/mL IFNγ and 100 ng/mL LPS for 6 h. The iNOS and

IL-1β protein expression were detected by Western blot and quantified by normalizing to GAPDH. *P < 0.05, **P < 0.01, n=4 (for panel B, D and H).